Polymer Degradation and Stability 123 (2016) 162–169

Contents lists available at ScienceDirect

Polymer Degradation and Stability

journal homepage: www.elsevier.com/locate/polydegstab

Influence of thermo-oxidative aging on the thermal conductivity of carbon fiber fabric reinforced epoxy composites

Wei Fan [a, b, *], Jia-lu Li [b], Yuan-yuan Zheng [b], Tian-jiao Liu [a], Xiao Tian [a], Run-jun Sun [a]

[a] Ministry of Education Key Laboratory of Functional Textile Material and Product, Xi'an Polytechnic University, Xi'an, Shaanxi 710048, China
[b] Ministry of Education Key Laboratory of Advanced Textile Composites, Tianjin Polytechnic University, Tianjin 300387, China

ARTICLE INFO

Article history:
Received 29 September 2015
Received in revised form
17 November 2015
Accepted 18 November 2015
Available online 22 November 2015

Keywords:
Polymer-matrix composite (PMC)
Carbon fiber fabric
Thermo-oxidative aging
Thermal conductivity
Weight loss

ABSTRACT

The present paper examined the thermo-oxidative aging (TOA) mechanism of the thermal conductivity of carbon fiber polymer composites (CF-PMCs) and the role of reinforced structure on the thermal conductivity of CF-PMCs under TOA conditions. The three dimensional and four directional braided carbon fiber/epoxy composites (BC), the laminated plain woven fabric/epoxy composites (LC), and the neat resins (NR) were investigated for up to 1200 h at 140 °C in air. The process resulted in progressive deterioration of the matrix rein and fiber/matrix interfaces, in the form of chain scissions, oxidization of carbon elements, weight loss, and cracks, which significantly led to the decrease of the thermal conductivity of the NR, LC, and BC. The ratio of fiber end area to the total surface area in a sample determined the rate of weight loss and the changes in thermal conductivity. The LC samples had 1.2 times higher ratio of fiber end area to the total surface area, and their loss in thermal conductivity and weight were significantly higher than that of BC samples at the same aging conditions. Besides, the thermal conductivity of CF-PMCs was highly negatively correlated with the weight loss under TOA conditions.
© 2015 Elsevier Ltd. All rights reserved.

1. Introduction

Carbon fiber polymer composites (CF-PMCs) are extensively employed in the aerospace industry owing to their high specific mechanical properties [1,2]. The thermal conductivity plays an important role in selecting the optimum materials to meet specific design requirements in many aerospace applications [3]. For example, leading edges in high-speed aircraft wings and inlet or exhaust areas of gas turbine engines are subject to localized thermal loads which must be transferred through the part thickness to adjacent cooler areas for subsequent convection, in part to mitigate internal stresses induced by reducing the thermal gradient across the part thickness [4]. Traditional laminated composites have low through-thickness thermal conductivities, which limit their use in a variety of aerospace applications. Three dimensional (3D) textile (braided, woven and stitched fabric) composites with the through-thickness CFs, by contrast, have a much higher thermal conductivity in the through-thickness [4,5].

No matter what kind of architectures is used to reinforce the polymer, oxidation reaction–diffusion phenomena must take place within PMCs when they are long exposed to elevated temperatures [6–10]. The process of thermal degradation has been studied for neat resins [10–12], CFs [13,14] but mainly for PMCs [8,9,15–17]. These studies have concentrated on the mechanism of thermo-oxidative degradation of the material. The thermal-oxidative aging (TOA) of polymer involves physical and chemical aging. Physical aging [18] refers to structural relaxation of the glassy state toward the metastable equilibrium amorphous state, and it is accompanied by the increase of glass transition temperature (*Tg*) and modulus of the epoxy system [19–21]. Chemical aging mainly includes chemical structure changes of polymer resulting from high temperature and oxygen. Many studies suggest that chemical reactions of epoxy resin during TOA mainly contains post-cure [22,23], carbonyl growth [24,25], and chain scission [18,23], which leads to the weight loss [26] and micro-cracks [27] of the matrix. CF-PMCs oxidation is primarily a surface reaction phenomenon and preferential oxidation occurs along the fiber direction in unidirectional composites [9,28,29]. The resin shrinkage and mismatch of thermal expansion coefficients of fiber and resin give rise to localized residual stress and damage and eventually lead to interface microcracks [30,31].

* Corresponding author. Ministry of Education Key Laboratory of Functional Textile Material and Product, Xi'an Polytechnic University, Xi'an, Shaanxi 710048, China.
E-mail address: fanwei@xpu.edu.cn (W. Fan).

http://dx.doi.org/10.1016/j.polymdegradstab.2015.11.016
0141-3910/© 2015 Elsevier Ltd. All rights reserved.

The extent of mechanical property deterioration as a consequence of TOA has been widely covered, examining properties of flexural strength and modulus [32], tensile strength [33], interlaminar shear strength [34], compressive strength [33,35], and impact strength [36]. Besides, the physical properties of CF-PMCs such as vibration damping characteristic [37], electrical conductivity [38] after TOA has been studied. However, there are no researches having been reported on the effect of TOA on the thermal conductivity of CF-PMCs until now. The previous study [39] indicates that the thermal conductivity will decrease with the increase of air void in CF-PMCs under normal temperature. Therefore, the thermal conductivity may be changed when the micro-cracks formed in CF-PMCs after TOA. As a consequence, the lack of reliable data for the thermal conductivity of CF-PMCs may hamper their wide utilization.

The purpose of the current investigation was to understand the TOA mechanism of the thermal conductivity of CF-PMCs, to identify the change rules of the thermal conductivity of CF-PMCs under TOA conditions, and to determine the role of reinforced structure (3D and four-directional (4Dir) braiding preform and laminated plain woven fabric) on the thermal conductivity of CF-PMCs before and after TOA. Therefore samples were thermally oxidized at 140 °C for various durations. After exposure to the high temperature, composites are characterized to: (1) determine their weight loss and changes in thermal conductivity at different exposure times; (2) understand the TOA mechanism of thermal conductivity; (3) observe the corresponding micro-cracks and surface damage; (4) understand the reinforced mechanism using the different reinforced structure.

2. Manufacturing and experimental procedures

2.1. Materials

T700-12K carbon fiber (Toray) was used for this study. An epoxy resin JC-02A based on diglycidyl ether of bisphenol A (Changshu Jaffa Chemical Co., Ltd.) with hardener JC-02B (improved methyl tetrahydrophthalic anhydride) and accelerant JC-02C (tertiary amine) was used for the matrix.

2.2. Sample preparation

The 3D-4Dir braided preforms were manufactured by the intertwining or orthogonal interlacing of four sets of yarns-braiders to form a 3D integral structures [40], and each one was directly braided to form a 3D sheet fabric with the size of 250 mm (length) × 25 mm (width) × 4 mm (thickness). The 3D-4Dir braided architecture is illustrated in Fig. 1a. It is characterized by almost all the braider yarns being offset at different angles between the in-plane and through-thickness directions, which can be seen clearly from the tracer yarn (colored yarns). The laminated plain woven fabric is illustrated in Fig. 1c.

The epoxy resin was JC-02A, JC-02C and JC-02C, mixing them together by weight ratio of 100:80:1, and then using RTM (the resin transfer molding) process to make the composites. The process involved placing the 3D-4Dir braided preforms and 10 pieces of plain woven carbon fiber fabric into their own mold, closing the molds, checking them for leaks, and heating them to 90 °C. Once the molds and the pipeworks connected to the molds were sufficiently heated, a vacuum of approximately 0.3 MPa was applied to the pipeworks, the molds and the resin trap were allowed to stabilize for 5 min, and then the resin was injected into the molds. The injection process was continued until a sufficient volume of resin was seen in the resin trap, to indicate that the molds had been completely filled with resin. The molds were isolated from the resin pot and the resin trap and then put into an air-circulating oven. The manufacturer recommended cure cycle was employed: the first step of the cure cycle was 2 h at 90 °C, followed by 1 h at 110 °C, with the final step being 6 h at 140 °C. The fiber volume fractions for the two composites were about 55%. The making process of neat resin (NR) samples was similar as that of 3D-4Dir braided carbon fiber/epoxy composites (BC) except that the vacuum pressure for NR was 0.1 MPa.

After curing, ultrasonic C-scans were performed to ensure that the samples were free of voids errors. Then the large pieces were cut into testing samples (40 mm × 25 mm × 4 mm) with a water-cooled diamond wheel saw. Finally, the samples for the BC and laminated plain woven fabric/epoxy composites (LC) are shown in Fig. 1b and d, respectively.

2.3. Accelerated aging experiments

The BC, LC and NR samples were isothermally aged at 140 °C for 168, 360, 720, and 1200 h in dry air. After being heated for a given aging time, the samples were removed and cooled in a desiccator to avoid moisture absorption. The samples were stored at 25 ± 3 °C for at least 24 h prior to testing.

2.4. Tests

2.4.1. Fourier transform infrared (FTIR) spectroscopy

The micro-attenuated total reflection FTIR spectroscopy was used to determine the functional characteristics of NR in the surface layer before and after ageing in wavenumbers ranging from 4000 to 400 cm^{-1}. Data acquisition was performed automatically using an interfaced computer and a standard software package.

2.4.2. X-ray photoelectron spectroscopy (XPS)

XPS was used to analyze surface chemical elements of NR before and after TOA. The XPS instrumentation used in this experiment was Thermo ESCALAB 250 XPS equipped with an Al-Ka monochromatized X-ray with a spot size of around 400 μm in diameter.

2.4.3. Surface morphology observation

The surface morphology of the composites was examined in a VHX-1000 3D microscopy system.

2.4.4. Weight loss measurement

An electronic balance with 0.1 mg accuracy was used for recording the weight loss of the composites. The testing method is detailed elsewhere [8].

2.4.5. Thermal conductivity measurement

Thermal conductivity of the LC, BC and, NR was measured with a TC 3010 apparatus (Xi'an Xiatech Electronic Technology Co. Ltd., China), in accordance with ASTM C1113/C1113 M-09. Thermal conductivity tests were conducted at 25 °C.

3. Results and discussions

3.1. Chemical analysis

Evidence of chemical aging was quickly observed through the discoloration of the NR samples throughout the aging process [12,29]. The size of the discoloration is dependent on aging time and aging temperature. Images of the neat resin samples after aging for different aging times at 140 °C are shown in Fig. 2a. It can be seen that the color changed significantly with the increase of aging time, from yellow to brown, to dark brown, and finally to black.

Polished cross-sections of the NR samples were inspected to

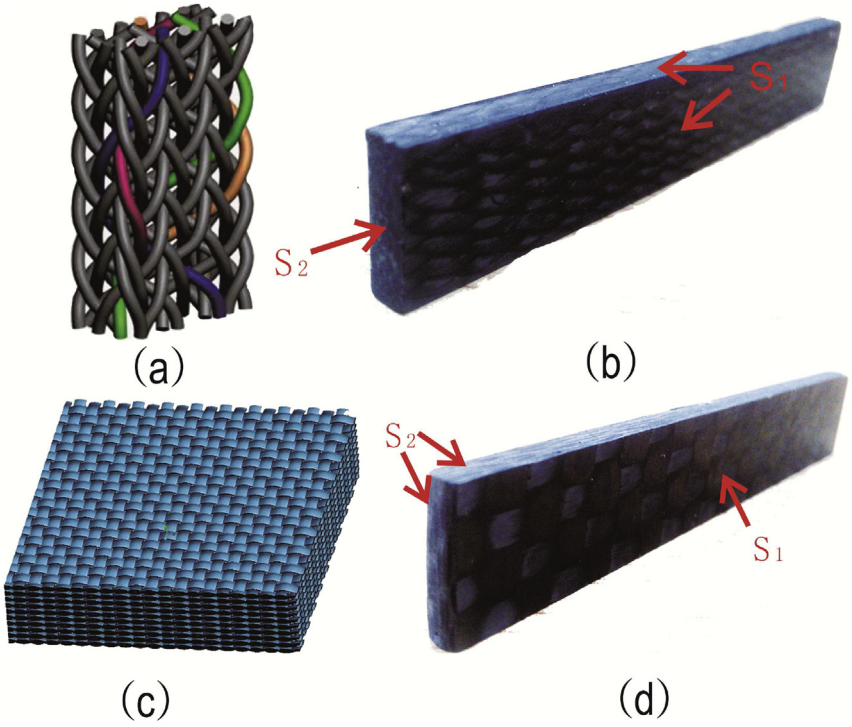

Fig. 1. Schematic of 3D-4Dir braided preform (a) and laminated plain weave fabric (c), and the corresponding composite: BC (b) and LC (d). S_1—Area of surfaces parallel to fiber direction, S_2—Area of surfaces perpendicular to fiber direction.

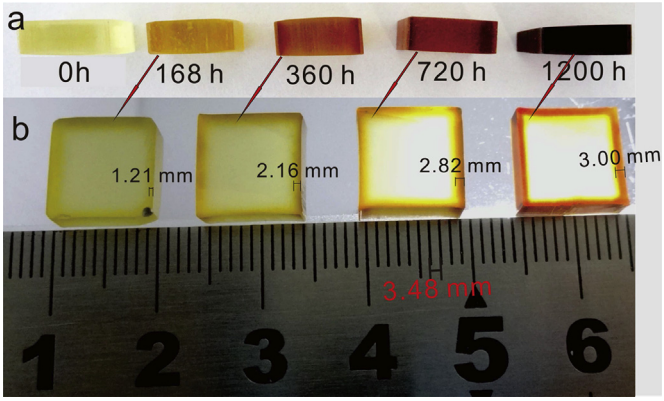

Fig. 2. Surface images (a) and the thicknesses of the oxidized layer (b) of the NR samples after aging for different aging times at 140 °C.

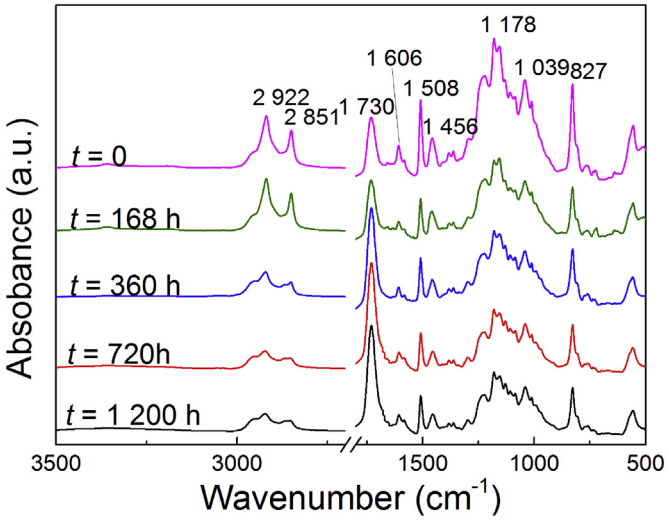

Fig. 3. FTIR spectra recorded on the surface of the un-aged and aged NR samples.

measure the thickness of the oxidized layer (TOL), as shown in Fig. 2b. Although the color change was drastic (Fig. 2a), the responsible chemical degradation was limited to the sample surface. The TOL of the samples aged for 168 h, 360 h, 720 h, and 1200 h at 140 °C were 0.32, 0.62, 0.81, and 0.86 mm, respectively. The TOL increased but the growth rate of TOL decreased with the increase of aging time.

The FTIR spectrometer was used to find out the reason for the discoloration of the NR samples during the aging process. The representative FTIR spectra of NR samples after aging at 140 °C for different aging times are shown in Fig. 3. It can be seen that the characteristic band of C=O near 1730 cm^{-1} increased with the decrease of the band of C–H near 2922 and 2851 cm^{-1}. The phenomena demonstrated that C–H bonds were oxidized and saturated aldehyde, ketone, ester, or acid was formed [10,33]. In addition, the characteristic absorption bands of benzene ring near 1606, 1508 and 1456 cm^{-1} decreased in intensity with aging process, which because the benzene ring structure was partly destroyed, and chemical species, O=(C_6H_4)=O (a 'black-color' element) [41] were formed. This is why the colors of the NR in the surface layer were changed under TOA condition. The absorption band near 1178 cm^{-1}, which derived from symmetrically stretching vibration of C–O-phenyl, decreased in intensity with the aging process. These results indicated that parts of C–O-phenyl were destroyed [33]. The intensity of carbonyl and C–H bonds did not appear to have obvious change from 720 h to 1200 h of the aging time. There may be two reasons for this phenomenon. Firstly, further oxidation of the carbonyl species was likely to form CO_2

with the aging proceeds [41]. Secondly, ketone formation yielded a structure more resistant to oxidation [27,42]. It is because the passive layer blocked diffusion of oxygen and protected the bulk epoxy from further oxidation, the growth rate of TOL decreased with the increase of aging time.

The XPS was used to quantitative analysis the effect of TOA on the surface element of NR, and the corresponding XPS spectra are presented in Fig. 4. The binding energies were referenced to the C1s and O1s lines at 284.8 eV 532 eV, respectively (Fig. 4). According to the XPS spectra peak area, the carbon and oxygen atom fraction can be calculated by the sensitivity normalization technique, and the corresponding results are shown in Table 1. From Table 1, it can be seen that the relative content of O and O/C increased with ongoing of aging time, especially after aging for 720 h, the percentage content of O/C reached 25.49%. However, the increase in the percentage content of O/C was almost negligible from 720 h to 1200 h. At the same time, the relative content of C had a decreasing trend overall, with the increase of aging time. There may be two reasons for the decrease of C. On the one hand, the parts of carbon functional groups were oxidized by O_2, resulting in the improving of O content and the decreasing of the C content; On the other hand, oxidation of the carbonyl species was likely to form CO_2, leaving the sample. The results are in agreement with those provided by FTIR.

3.2. Surface appearance analysis

Fig. 5 and Fig. 6 show the cross-section photomicrograph of LC and BC samples after aged at 140 °C for 1200 h compared to the unaged ones, respectively. No damage was observed on the unaged sample surfaces (Figs. 5a and 6a). However, a lot of micro-cracks appeared on the aged samples (Figs. 5b and 6b). The white fiber bundles were parallel to the surface, and the dark fiber bundles were perpendicular to the surface (Fig. 5). From Fig. 5c, it can be seen that the micro-cracks largely appeared on the fiber end areas and few on the areas parallel to the fiber, which was because the axial propagation of the oxidation along the CF was dramatically greater than the oxidation in the transverse direction [28].

3.3. Weight loss analysis

Fig. 7 illustrates the measured weight loss of the two composites at 140 °C as a function of aging time. It can be seen that the weight loss all increased with longer aging times. Besides, the weight loss of LC was about 1.35 times as high as that of BC.

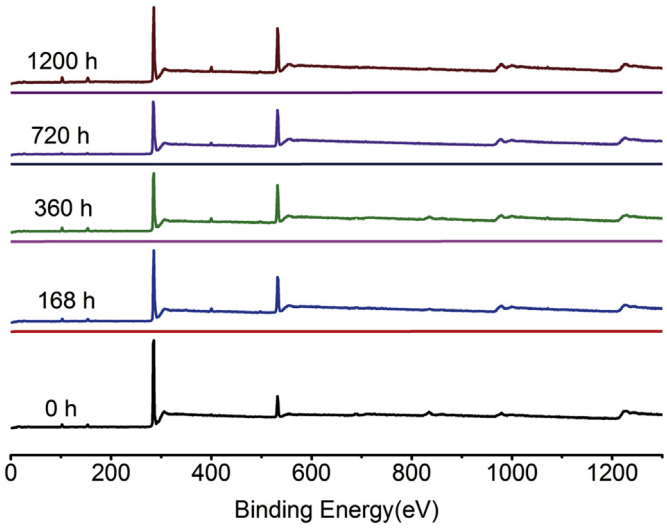

Fig. 4. XPS spectra recorded on the surface of un-aged and aged NR samples.

Table 1
The content of C, O and the ratio of O/C on the un-aged and aged NR sample surfaces.

Element content(%)	Aging time(h)				
	0	168	360	720	1200
C	82.5	74.97	69.88	76.11	71.61
O	8.38	17.19	17.25	19.40	18.26
O/C	10.16	22.93	24.69	25.49	25.50

In the case of CF-PMCs, weight loss was (in general) associated only with the polymer, as the CF was thermally stable at 140 °C [41]. In this research, the LC and BC samples owned the same matrix resin content (45%), so they should have the same weight loss. The weight loss of the two composites did not appear to follow the expected behavior with the weight loss of BC equal to that of the LC, however, the LC lost considerably more weight than BC under the same aging conditions. It was because the surfaces of samples with different microstructural characteristics were expected to exhibit different oxidation behavior. A sample with higher percentage of fiber end area exposed to air is more susceptible to lead interface oxidation, resulting in more weight loss [9,28]. In this article, the surface area ratio $S_2/(S_1 + S_2)$ for LC and BC was 20.6% and 7.9%, respectively. The plain weave fabric only had half of the fibers perpendicular to S_2, so the actual ratio of fiber end area to the total surface area in LC was 10.3%, which was about 1.2 times higher than that of in BC. Therefore, the LC lost more weight than BC.

3.4. Thermal conductivity analysis

The transient hot-wire method can be free from the effect of natural convection due to its promptness in the measurement [43]. It allows the identification of the transverse thermal conductivity as a function of temperature of dry preform and cured composites [44]. Therefore, the transient hot-wire method was used to measure the thermal conductivity of the NR, BC and LC in this study. Fig. 8a and b shows the experimental set up for testing samples and the measurement model of the hot wire method, respectively. The sample-1 is basically the same as the sample-2 (Fig. 8).

Table 2 shows thermal conductivity of the NR, LC, and BC before and after TOA. From Table 2, it can be seen that the average thermal conductivity of the unaged NR, LC, and BC was 0.1825, 1.329, and 0.913 $W\ m^{-1}\ K^{-1}$, respectively. The transverse thermal conductivity of LC was about 1.45 times higher than that of BC although they have the same CF volume fractions. This is because the axial thermal conductivity of CFs was 9 times the high of the radial thermal conductivity, making highly anisotropic thermal behavior of CF-PMCs [44]. For LC, there were 50% of continuous CFs in the transverse direction, by contrast, there were no continuous CFs for BC in this direction, so the average thermal conductivity of LC was bigger than that of BC.

In order to compare the difference of TOA effect on the thermal conductivity of the NR, LC, and BC, the normalization method was used to process the data in Table 2, the corresponding results are shown in Fig. 9. It can be seen that the thermal conductivity of the NR, LC, and BC all decreased with the increasing of aging time. At the same time, however, the thermal conductivity retention rates of the three materials were difference. Among them, the thermal conductivity retention rate of NR was the highest, and the LC was the lowest.

There may be two reasons for the decrease in thermal conductivity for NR, LC and BC after TOA.

On the one hand, the high thermal conductivity carbon element

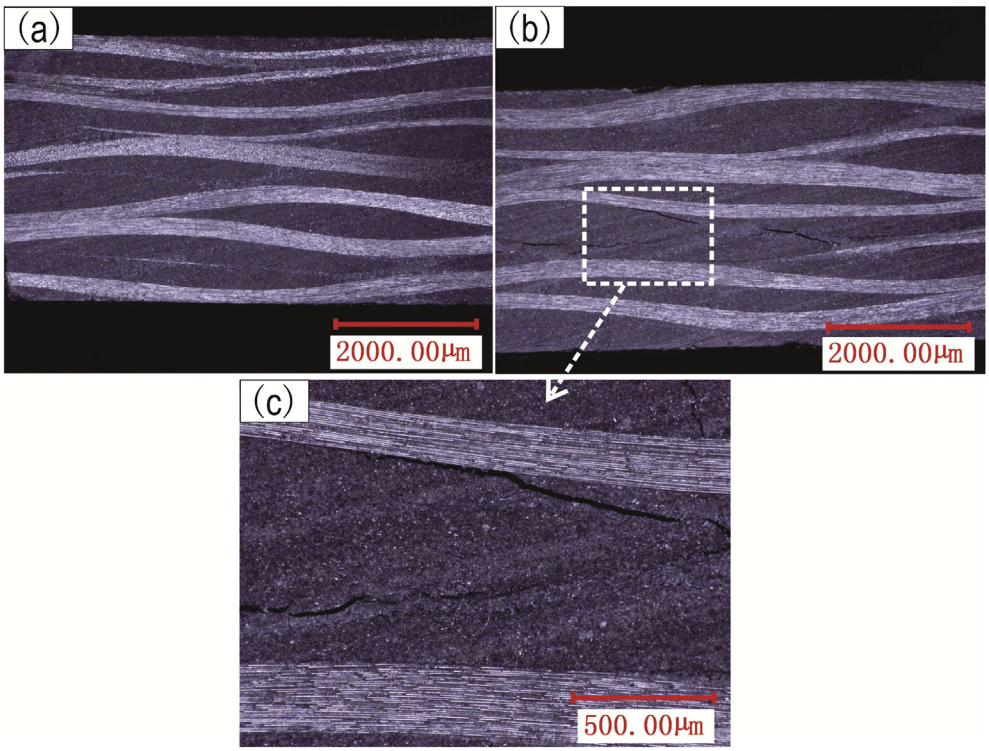

Fig. 5. The cross-sectional photomicrographs of the (a) un-aged and (b) aged (140 °C-1200 h) LC samples. (c) Zoom on thermo-oxidation induced micro-cracks corresponding to (b).

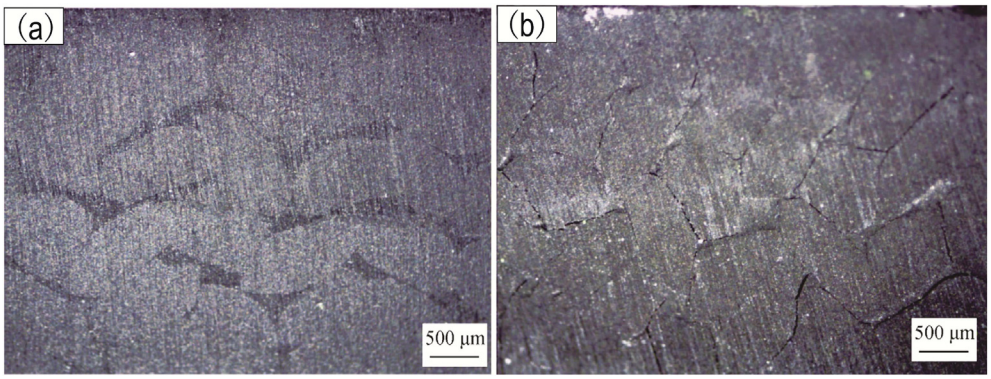

Fig. 6. The cross-sectional photomicrographs of (a) un-aged and (b) aged (140 °C-1200 h) BC samples.

decreased and the low thermal conductivity oxygen element increased on the sample surface after TOA; On the other hand, the voids and cracks were formed in the matrix and fiber/matrix interfaces, filling by the air. The thermal conductivity of the air void is taken to be 0.0242 W m^{-1} K^{-1} [39], which was lower than that of epoxy resin and CF, so the thermal conductivity decreased after TOA. The reason for the lower thermal conductivity retention rate in LC and BC than that of NR was that the CF/matrix interfaces of the composites degraded due to the resin shrinkage and mismatch of thermal expansion coefficients of CF and matrix resin [45], forming more cracks than the NR.

The cracks were highly positively correlated with weight loss [27]. Therefore, the LC lost considerably more weight than BC under the same aging conditions that means more cracks were formed in LC than in BC. The cracks in PMCs can result in the decrease of their thermal conductivity, so we can indirectly come to the conclusion that the more weight loss of PMCs the more thermal conductivity loss was. In order to prove the correctness of the inference, the linear regression analysis method was used to process the data between the weight loss and the thermal conductivity of LC and BC, the analysis results are shown in Fig. 10. It can be seen that the thermal conductivity decreased with the increase of the weight loss of LC and BC. Besides, the R^2 (correlation coefficient square) for LC (Fig. 10a) and BC (Fig. 10b) was 0.93 and 0.99, respectively. It showed that the thermal conductivity for PMCs was highly negatively correlated with the weight loss. It can reasonably explain why the thermal conductivity retention rate of LC was lower than that of BC at the same aging conditions.

4. Conclusions

The present paper examined the thermo-oxidative aging (TOA) mechanism of the thermal conductivity for carbon fiber polymer composites (CF-PMCs) and the role of reinforced structure (three-

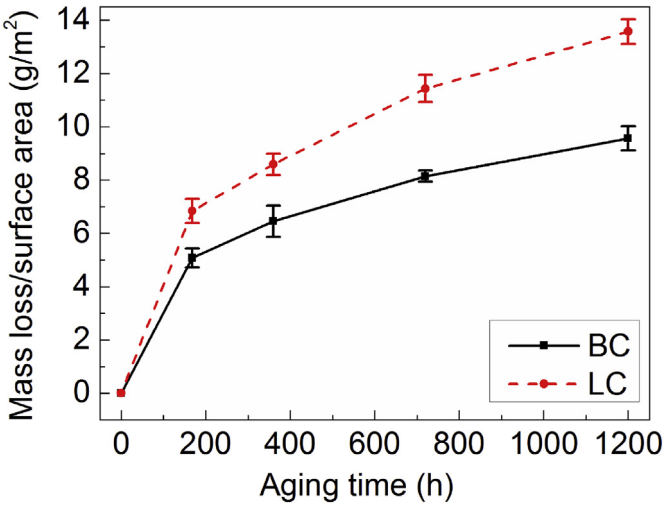

Fig. 7. Weight loss per surface area vs. aging time for the BC and LC samples aged at 140 °C.

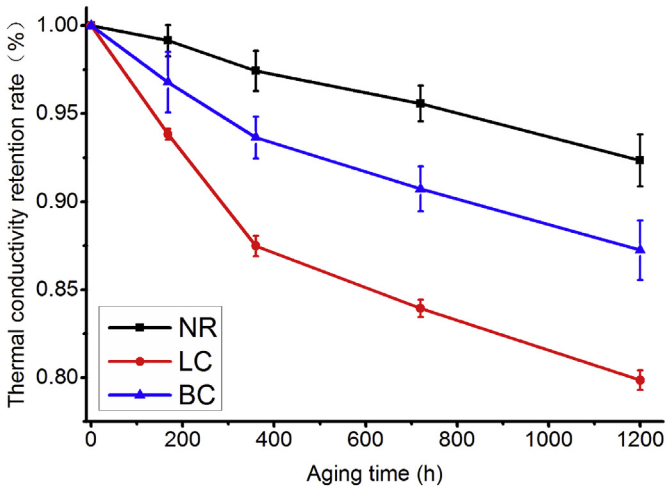

Fig. 9. Thermal conductivity retention rate of NR, LC and BC samples vs. aging time at 140 °C.

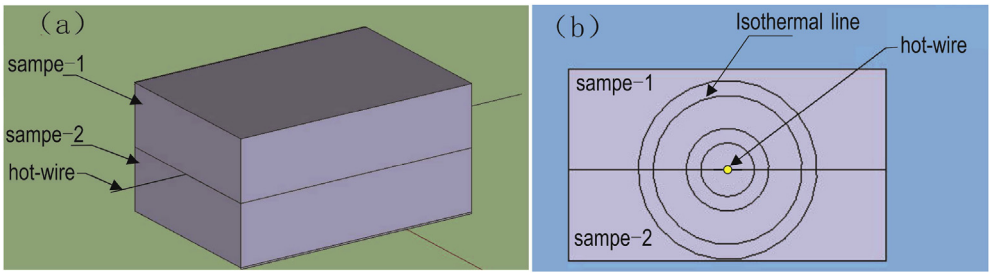

Fig. 8. The experimental set up for testing samples (a) and the measurement model (b) of hot wire method.

Table 2
Thermal conductivity of un-aged and aged NR, LC and BC samples.

Material	Aging time(h)	Thermal conductivity (W m^{-1} K^{-1})						
		1#	2#	3#	4#	5#	Average	Standard deviation
NR samples	0	0.1820	0.1821	0.1819	0.1837	0.1827	0.1825	0.00075
	168	0.1805	0.1804	0.1811	0.1808	0.1818	0.1809	0.00056
	360	0.1783	0.1783	0.1783	0.1759	0.1780	0.1778	0.00106
	720	0.1732	0.1740	0.1743	0.1750	0.1755	0.1744	0.00089
	1200	0.1683	0.1676	0.1696	0.1675	0.1696	0.1685	0.00103
LC samples	0	1.334	1.344	1.330	1.338	1.302	1.329	0.01627
	168	1.253	1.249	1.232	1.263	1.241	1.248	0.01178
	360	1.165	1.178	1.140	1.175	1.158	1.163	0.01522
	720	1.112	1.101	1.108	1.135	1.124	1.116	0.01351
	1200	1.056	1.065	1.061	1.036	1.091	1.062	0.01977
BC samples	0	0.9181	0.9233	0.8946	0.9167	0.9121	0.9130	0.01101
	168	0.8993	0.8731	0.8626	0.8870	0.8961	0.8836	0.01554
	360	0.8393	0.8512	0.8681	0.8613	0.8547	0.8549	0.01087
	720	0.8183	0.8193	0.8472	0.8264	0.8301	0.8283	0.01168
	1200	0.8151	0.8015	0.7805	0.8051	0.7806	0.7966	0.01545

dimensional and four-directional braiding preform and laminated plain woven fabric) on the thermal conductivity of CF-PMCs before and after TOA. Before TOA, the average thermal conductivity of the unaged neat resin (NR), laminated plain woven fabric/epoxy composites (LC), and the three dimensional and four directional braided carbon fiber/epoxy composites (BC) was 0.1825, 1.329, and 0.913 W m^{-1} K^{-1}, respectively. The transverse thermal conductivity of LC was about 1.45 times higher than that of BC due to more continuous CFs in the transverse direction for LC than for BC. After aging at 140 °C for various durations (up to 1200 h), the thermal conductivity of the NR, LC, and BC all decreased with the increasing of aging time. There may be two reasons for the decrease in thermal conductivity for NR, LC and BC after TOA. On the one hand, the high thermal conductivity carbon element decreased and the low thermal conductivity oxygen element increased on the sample surface after TOA; On the other hand, the voids and cracks in the matrix and fiber/matrix interfaces were filled by the air with low thermal conductivity (0.0242 W m^{-1} K^{-1}). At the same aging conditions, the thermal conductivity retention rates of LC and BC were lower than that of NR, which was because the CF/matrix interfaces of the

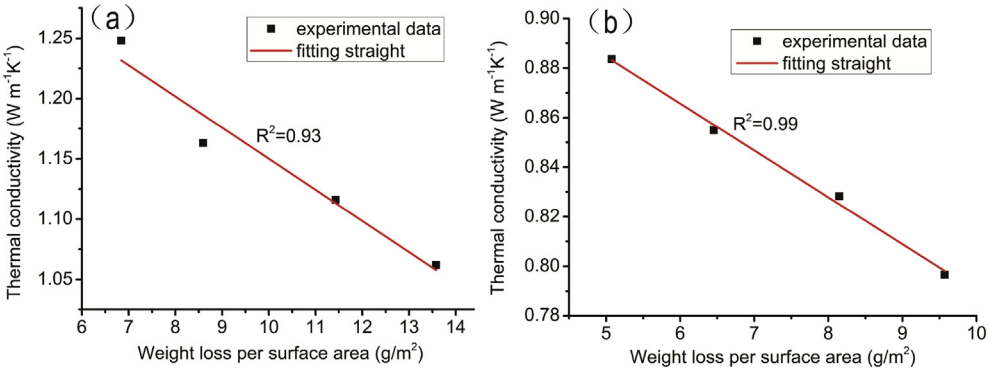

Fig. 10. The thermal conductivity vs. the weight loss of LC and BC samples.

composites degraded due to the resin shrinkage and mismatch of thermal expansion coefficients of CF and matrix resin, forming more cracks than the NR. The ratio of fiber end area to the total surface area in a sample determined the rate of weight loss. The LC samples, having 1.2 times higher ratio of fiber end area to the total surface area, have shown 1.35 times the weight loss at the same aging conditions, compared to the BC samples. The thermal conductivity of PMCs was highly negatively correlated with the weight loss, so the LC lost much more thermal conductivity than BC at the same aging conditions.

Acknowledgment

The authors wish to acknowledge the sponsorship of Research Fund for the Doctoral Program of Xi'an Polytechnic University, China (Nos. BS1514) and Cooperative Innovational Center for Technical Textiles,Shaanxi Province (Nos. 2015ZX-02).

References

[1] H. Rahmani, S.H.M. Najafi, A. Ashori, Mechanical performance of epoxy/carbon fiber laminated composites, J. Reinf. Plast. Compos. 33 (8) (2014) 733–740.
[2] X.L. Yang, Z.C. Wang, M.Z. Xu, R. Zhao, X.B. Liu, Dramatic mechanical and thermal increments of thermoplastic composites by multi-scale synergetic reinforcement: carbon fiber and graphene nanoplatelet, Mater. Des. 44 (2013) 74–80.
[3] F.A. Al-Sulaiman, Y.N. Al-Nassar, E.M.A. Mokheimer, Prediction of the thermal conductivity of the constituents of fiber-reinforced composite laminates: voids effect, J. Compos. Mater. 40 (9) (2006) 797–814.
[4] J. Schuster, D. Heider, K. Sharp, M. Glowania, Thermal conductivities of three-dimensionally woven fabric composites, Compos. Sci. Technol. 68 (9) (2008) 2085–2091.
[5] H.J. Xu, L.T. Zhang, Y.G. Wang, L.F. Cheng, The effects of Z-stitching density on thermophysical properties of plain woven carbon fiber reinforced silicon carbide composites, Ceram. Int. 41 (1) (2015) 283–290.
[6] T.K. Tsotsis, S.M. Lee, Long-term thermo-oxidative aging in composite materials: failure mechanisms, Compos. Sci. Technol. 58 (3–4) (1998) 355–368.
[7] D.Q. Vu, M. Gigliotti, M.C. Lafarie-Frenot, The effect of thermo-oxidation on matrix cracking of cross-ply 0/90 (S) composite laminates, Compos. Part A 44 (2013) 114–121.
[8] W. Fan, J.L. Li, Rapid evaluation of thermal aging of a carbon fiber laminated epoxy composite, Polym. Compos. 35 (5) (2014) 975–984.
[9] M.H. Haque, P. Upadhyaya, S. Roy, T. Ware, W. Voit, H. Lu, The changes in flexural properties and microstructures of carbon fiber bismaleimide composite after exposure to a high temperature, Compos. Struct. 108 (2014) 57–64.
[10] Y.M. Pei, K. Wang, M.S. Zhan, W. Xu, X.J. Ding, Thermal-oxidative aging of DGEBA/EPN/LMPA epoxy system: chemical structure and thermal-–mechanical properties, Polym. Degrad. Stab. 96 (7) (2011) 1179–1186.
[11] H. Luo, G. Lu, S. Roy, H. Lu, Characterization of the viscoelastic behavior of bismaleimide resin before and after exposure to high temperatures, Mech. Time Depend. Mater. 17 (3) (2013) 369–399.
[12] S.G. Miller, G.D. Roberts, J.L. Bail, L.W. Kohlman, W.K. Binienda, Effects of hygrothermal cycling on the chemical, thermal, and mechanical properties of 862/W epoxy resin, High Perform. Polym. 24 (6) (2012) 470–477.
[13] K.J. Bowles, G. Nowak, Thermo-oxidative stability studies of Celion 6000/PMR-15 unidirectional composites, PMR-15, and Celion 6000 fiber, J. Compos. Mater. 22 (10) (1988) 966–985.
[14] M. Wong, A. Skontorp, S. Wang, Thermal oxidation of carbon fibers and carbon-fiber reinforced high-temperature polyimide composite at elevated temperatures, Proc. Am. Soc. Compos. Tech. Publ. AG (1994) 458.
[15] J. Liu, X. Zhu, Z. Zhou, L. Wu, L. Ma, Effects of thermal exposure on mechanical behavior of carbon fiber composite pyramidal truss core sandwich panel, Compos. Part B 60 (2014) 82–90.
[16] D.Q. Vu, M. Gigliotti, M.C. Lafarie-Frenot, Experimental characterization of thermo-oxidation induced shrinkage and damage in polymer-matrix composites, Compos. Part A 43 (4) (2012) 577–586.
[17] X.Y. Lv, R.G. Wang, W.B. Liu, L. Jiang, Effect of thermal-oxidative aging on carbon fibre-bismaleimide composites, Pigment Resin Technol. 41 (1) (2012) 34–41.
[18] D. Leveque, A. Schieffer, A. Mavel, J.F. Maire, Analysis of how thermal aging affects the long-term mechanical behavior and strength of polymer–matrix composites, Compos. Sci. Technol. 65 (3) (2005) 395–401.
[19] J.L. Fuente, An analysis of the thermal aging behaviour in high-performance energetic composites through the glass transition temperature, Polym. Degrad. Stab. 94 (4) (2009) 664–669.
[20] L. Barral, J. Cano, J. Lopez, I. Lopez-Bueno, P. Nogueira, M.J. Abad, C. Ramírez, Physical aging of a tetrafunctional/phenol novolac epoxy mixture cured with diamine DSC and DMA measurements, J. Therm. Anal. Calorim. 60 (2) (2000) 391–399.
[21] L. Barral, J. Cano, J. Lopez, I. Lopez-Bueno, P. Nogueira, M.J. Abad, C. Ramirez, Physical aging of an epoxy/cycloaliphatic amine resin, Eur. Polym. J. 35 (3) (1999) 403–411.
[22] A. Cherdoud-Chihani, M. Mouzali, M.J.M. Abadie, Study of crosslinking AMS/DGEBA system by FTIR, J. Appl. Polym. Sci. 69 (6) (1998) 1167–1178.
[23] Wei Fan, J.L. Li, D.D. Guo, Effect of thermo-oxidative aging on three-dimensional and four-directional braided carbon fiber/epoxy composite, J. Compos. Mater. (2014), http://dx.doi.org/10.1177/0021998314561067.
[24] B. Dao, J. Hodgkin, J. Krstina, J. Mardel, W. Tian, Accelerated aging versus realistic aging in aerospace composite materials. V. The effects of hot/wet aging in a structural epoxy composite, J. Appl. Polym. Sci. 115 (2) (2010) 901–910.
[25] J. Decelle, N. Huet, V. Bellenger, Oxidation induced shrinkage for thermally aged epoxy networks, Polym. Degrad. Stab. 81 (2) (2003) 239–248.
[26] C. Zhang, W.K. Binienda, G.N. Morscher, R.E. Martin, L.W. Kohlman, Experimental and FEM study of thermal cycling induced microcracking in carbon/epoxy triaxial braided composites, Compos. Part A 46 (2013) 34–44.
[27] M.A.B. Meador, C.E. Lowell, P.J. Cavano, P. Herrera-Fierro, On the oxidative degradation of nadic endcapped polyimides: I. Effect of thermocycling on weight loss and crack formation, High Perform. Polym. 8 (3) (1996) 363–379.
[28] G. Schoeppner, G. Tandon, E. Ripberger, Anisotropic oxidation and weight loss in PMR-15 composites, Compos. Part A 38 (3) (2007) 890–904.
[29] T. Tsotsis, Thermo-oxidative aging of composite materials, J. Compos. Mater. 29 (3) (1995) 410–422.
[30] K. Pochiraju, G. Tandon, G. Schoeppner, Evolution of stress and deformations in high-temperature polymer matrix composites during thermo-oxidative aging, Mech. Time Depend. Mater. 12 (1) (2008) 45–68.
[31] M.C. Lafarie-Frenot, S. Rouquie, Influence of oxidative environments on damage in c/epoxy laminates subjected to thermal cycling, Compos. Sci. Technol. 64 (10–11) (2004) 1725–1735.
[32] M. Akay, G. Spratt, Evaluation of thermal ageing of a carbon fibre reinforced bismalemide, Compos. Sci. Technol. 68 (15) (2008) 3081–3086.
[33] J. Wolfrum, S. Eibl, L. Lietch, Rapid evaluation of long-term thermal degradation of carbon fibre epoxy composites, Compos. Sci. Technol. 69 (3) (2009) 523–530.
[34] W. Fan, J.L. Li, Y.Y. Zheng, Improved thermo-oxidative stability of three-dimensional and four-directional braided carbon fiber/epoxy hierarchical composites using graphene-reinforced gradient interface layer, Polym. Test. 44 (2015) 177–185.
[35] H.Y. Luo, S. Roy, H.B. Lu, Dynamic compressive behavior of unidirectional IM7/

5250-4 laminate after thermal oxidation, Compos. Sci. Technol. 72 (2) (2012) 159–166.
[36] W. Fan, J.L. Li, H. Wang, D.D. Guo, Influence of thermo-oxidative aging on the impact property of conventional and graphene-based carbon fabric composites, J. Reinf. Plast. Compos. 34 (2) (2015) 116–130.
[37] W. Fan, J.L. Li, L. Chen, H. Wang, D.D. Guo, J.X. Liu, Influence of thermo-oxidative aging on vibration damping characteristics of conventional and graphene-based carbon fiber fabric composites, Polym. Compos. (2015), http://dx.doi.org/10.1002/pc.23484.
[38] E. Dalas, S. Sakkopoulos, E. Vitoratos, Thermal degradation of the electrical conductivity in polyaniline and polypyrrole composites, Synth. Met. 114 (3) (2000) 365–368.
[39] Y.N. Al-Nassar, Prediction of thermal conductivity of air voided-fiber-reinforced composite laminates part II: 3D simulation, Heat Mass Transf. 43 (2) (2006) 117–122.
[40] X. Sun, C.J. Sun, Mechanical properties of three-dimensional braided composites, Compos. Struct. 65 (3–4) (2004) 485–492.
[41] S. Ohno, M.H. Lee, K.Y. Lin, F.S. Ohuchi, Thermal degradation of IM7/BMI5260 composite materials: characterization by X-ray photoelectron spectroscopy, Mater. Sci. Eng. A 293 (1–2) (2000) 88–94.
[42] A. Lowe, B. Fox, V. Otieno-Alego, Interfacial ageing of high temperature carbon/bismaleimide composites, Compos. Part A 33 (10) (2002) 1289–1292.
[43] C. Da Hee, L. Juhyuk, H. Hiki, K. Yong Tae, Thermal conductivity and heat transfer performance enhancement of phase change materials (PCM) containing carbon additives for heat storage application, Int. J. Refrig. 42 (2014) 112–120.
[44] M. Villiere, D. Lecointe, V. Sobotka, N. Boyard, D. Delaunay, Experimental determination and modeling of thermal conductivity tensor of carbon/epoxy composite, Compos. Part A 46 (2013) 60–68.
[45] W. Fan, J.L. Li, Thermo-oxidative aging mechanism of carbon fiber reinforced polymer matrix composites, J. Solid Rocket Technol. 38 (1) (2015) 116–122 and 40.